ADVANCING EARTH AND SPACE SCIENCES

JGR Solid Earth

RESEARCH ARTICLE

10.1029/2025JB033219

Block Kinematics, Interseismic Coupling and Fault Slip Rates in the Aegean Region From GPS and Earthquake Slip Vector Data: 2. Hellenic Subduction System

Konstantinos Chousianitis[1], Volkan Özbey[2], Sotiris Sboras[1], Robert McCaffrey[3], and Semih Ergintav[4]

[1]Institute of Geodynamics, National Observatory of Athens, Athens, Greece, [2]Department of Geomatics Engineering, Istanbul Technical University, Istanbul, Turkey, [3]Department of Geology, Portland State University, Portland, OR, USA, [4]Geodesy Department, Bogazici University, Kandilli Observatory and Earthquake Research Institute, Istanbul, Turkey

Key Points:

- We examine the interseismic locking pattern on the Hellenic subduction system and quantify its spatial variability
- Our data indicate greater strain accumulation in the western Hellenic subduction system than in the eastern
- Low- to moderately locked sections can exhibit different slip behavior and release accumulated strain via earthquakes or aseismic slip

Supporting Information:

Supporting Information may be found in the online version of this article.

Correspondence to:

K. Chousianitis,
chousianitis@noa.gr

Citation:

Chousianitis, K., Özbey, V., Sboras, S., McCaffrey, R., & Ergintav, S. (2026). Block kinematics, interseismic coupling and fault slip rates in the Aegean region from GPS and earthquake slip vector data: 2. Hellenic subduction system. *Journal of Geophysical Research: Solid Earth*, *131*, e2025JB033219. https://doi.org/10.1029/2025JB033219

Received 17 OCT 2025
Accepted 24 MAY 2026

Author Contributions:

Conceptualization: Konstantinos Chousianitis
Data curation: Konstantinos Chousianitis, Semih Ergintav
Investigation: Konstantinos Chousianitis, Sotiris Sboras
Methodology: Konstantinos Chousianitis, Volkan Özbey, Robert McCaffrey
Software: Konstantinos Chousianitis, Volkan Özbey, Robert McCaffrey
Supervision: Konstantinos Chousianitis
Visualization: Konstantinos Chousianitis
Writing – original draft: Konstantinos Chousianitis

Abstract

The Hellenic subduction system is the primary locus of Nubia-Eurasia convergence, yet the distribution of strain accumulation along it is still debated. Here, we invert 832 geodetic velocities and 146 earthquake slip vectors to assess the spatial variability of interseismic locking and provide new constraints on the rate of slip deficit accumulation. We find that the subduction interface beneath southwestern Peloponnese and across the area from offshore south Peloponnese to offshore southwest of western Crete hosts three patches of low to moderate locking (0%–40%) at 10–50 km depth whose slip rate deficits account for ∼15–30% of the total plate convergence. The offshore weakly locked patches show a good spatial correlation with large interplate earthquakes, while the patch beneath southwestern Peloponnese overlaps with a past transient slow-slip event, suggesting that similarly locked areas along the interface can exhibit different slip behavior. Our analysis further reveals that the Hellenic Trough fault displays a low-coupled area that spatially correlates with the coseismic slip of the 365AD Crete earthquake and also identifies a confined region offshore of Gavdos island exhibiting higher degrees of locking. Finally, our modeling indicates that the eastern Hellenic subduction system is completely uncoupled, highlighting a fundamental difference with the heterogeneous locking of the western part. This work demonstrates that although most of the Nubia/Eurasia convergence is accommodated aseismically, localized patches prone to accumulating elastic strain do exist and it provides, for the first time, evidence for a connection between interseismic locking and large subduction-related earthquakes along the Hellenic subduction system.

Plain Language Summary

The Hellenic subduction zone, where the African (Nubian) plate moves beneath the Eurasian plate, is one of the most active tectonic regions in the Mediterranean. However, it remains unclear how and where strain builds up along this plate boundary. In this study, we combine GPS velocities and earthquake data to locate where and how strongly parts of the subduction zone are stuck (or "locked") and may store elastic strain. We find that along the western Hellenic subduction zone, from southwest Peloponnese to southwest Crete, there are three main areas where the plates are partially locked, with 15%–30% of the total plate motion stored as strain that could eventually be released. Two of these areas coincide with locations of past large earthquakes and one with a past slow-slip event (i.e., when the fault slips gradually rather than suddenly), suggesting that regions with similar locking can behave in different ways, releasing strain either seismically or aseismically. In contrast, the eastern Hellenic subduction zone appears to experience creep, meaning that the plates there are constantly, slowly slipping. Our results show that while most of the plate motion between Africa and Eurasia occurs aseismically, certain regions can accumulate strain and host large subduction-related earthquakes.

1. Introduction

The Hellenic subduction system represents a complex plate boundary zone in eastern Mediterranean where the northward moving Nubian plate subducts beneath an internally deforming Aegean plate that moves toward the SW. Convergence occurs at a rate of ∼35 mm/yr, which greatly exceeds the much slower convergence rate of ∼6 mm/yr between Nubia and Eurasia (McClusky et al., 2000; Reilinger et al., 2006). This considerable difference is attributed to the rapid movement of the Aegean plate, which induces slab rollback and trench retreat along the Hellenic subduction system (Brun & Sokoutis, 2010; Jolivet et al., 2013; Meijer & Wortel, 1997; Royden, 1993; van Hinsbergen & Schmid, 2012). The western termination of the Hellenic subduction system is

Writing – review & editing: Volkan Özbey, Sotiris Sboras, Robert McCaffrey, Semih Ergintav

the dextral Cephalonia Transform Fault Zone (CTFZ) which marks the transition from oceanic subduction across the Hellenic Arc, to continental collision with the simultaneous presence of ongoing active subduction of continental lithosphere across NW Greece (Pearce et al., 2012; Royden & Papanikolaou, 2011; Suckale et al., 2009). The eastern termination of the Hellenic subduction system is located beneath southwestern Anatolia where a major vertical or subvertical tear in the Nubian lithosphere separates the Hellenic and Cyprus Arcs (de Boorder et al., 1998; Kounoudis et al., 2020; Piromallo & Morelli, 2003; Schildgen et al., 2014; van Hinsbergen et al., 2010). This tear is associated with absence of intermediate depth earthquakes and its width increases with depth (Biryol et al., 2011; Bocchini et al., 2018).

Plate convergence across the Hellenic subduction system becomes increasingly oblique from west to east, as a result of its highly curved geometry. In this context, west of Crete convergence is almost frontal, while from eastern Crete to Rhodes, the Nubian-Aegean relative motion is largely oblique to the Hellenic Arc, inducing sinistral reverse movements across large en-echelon structures (Bocchini et al., 2018; Meier et al., 2007; Özbakır et al., 2013; ten Veen & Kleinspehn, 2003). Local and regional seismicity, wide-aperture seismic data and receiver function data have been used to constrain the shape of the subducting Nubian slab, which looks like a curved cone whose dip angle progressively increases with depth (Bocchini et al., 2018; Ganas & Parsons, 2009; Gudmundsson & Sambridge, 1998; Hayes et al., 2018; Papazachos et al., 2000). The downgoing slab exhibits a first-order segmentation at its eastern part due to the presence of a double Wadati-Benioff zone (Bocchini et al., 2018) and undergoes internal deformation which is verified by intraslab earthquakes with compression (P) axes oriented parallel to the strike of the subduction (Benetatos et al., 2004; Bocchini et al., 2018; Shaw & Jackson, 2010). Interplate seismicity across the Hellenic subduction system is characterized by low-angle thrust focal mechanisms with depths up to 45 km (Benetatos et al., 2004; Shaw & Jackson, 2010; Taymaz et al., 1990).

Historical as well as instrumental data highlight that these events generally do not exceed M_w 7.0 and, contrary to what is usually observed at other subduction zones, great earthquakes above M_w 8.0 are extremely rare and are only reported in historical records. These records suggest the occurrence of one M_w 8.3–8.5 earthquake to the SW of Crete in 365 AD and one $\sim M_w$ 8 somewhere between SE Crete and Rhodes in 1303 AD (Ambraseys, 2009; Guidoboni & Comastri, 1997). However, both of these historical events have been associated with ruptures on steep upper plate splay faults and not with the main subduction zone interface (Howell et al., 2015; Mouslopoulou et al., 2015; Shaw et al., 2008; Vernant et al., 2014). In that case, the absence of the typical great megathrust earthquakes implies a largely aseismic subduction where the observed $M_w < 7.0$ interplate events occur after the release of accumulated elastic strain at small-sized locked areas of the plate interface.

The coexistence of rapid convergence and limited seismic release makes the Hellenic subduction system a compelling example of the complex behavior observed at subduction plate boundaries. Globally, such settings comprise geodynamic environments which attract wide research interest among geoscientists of various disciplines since they are directly responsible for increased hazard and risk associated with various subduction-related natural disasters such as earthquakes, tsunamis and volcanic eruptions (McGuire et al., 2017; Wirth et al., 2022). The wealth of data which is recorded by dense monitoring networks that operate above many of these convergent margins has contributed to the development of new methods and approaches to model subduction processes and understand their dynamics (Brudzinski & Allen, 2007; Dragert et al., 2001; Fujiwara et al., 2011; McCaffrey, 2009; McCaffrey et al., 2000; Rondenay et al., 2008; Saffer & Tobin, 2011; Wallace, 2005). Especially when it comes to crustal deformation, seismogenesis and earthquake hazard associated with subduction zones, geodetic monitoring has become fundamental in providing first-order constraints on subduction kinematics and dynamics (Bock & Melgar, 2016; Murray-Moraleda, 2009). To this end, dense velocity fields and long coordinate time series obtained from continuously operating stations of Global Positioning System (GPS) networks have been used to measure the elastic strain accumulation at subduction zones which is expected to be released either during the coseismic and postseismic phases of future large earthquakes or as slow-slip events (Bürgmann et al., 2005; Cosenza-Muralles et al., 2022; Elliott & Freymueller, 2020; McCaffrey, 2014; Métois et al., 2012; Ohta et al., 2004; Wallace et al., 2004, 2012). The degree that the plate interface accumulates strain can be quantified by comparing the long-term relative motion rate (i.e., over many seismic cycles) with the short-term rate (i.e., during the interseismic period). The latter is expected either to be equal to the long-term plate motion rate if the interface accommodates the entire amount of convergence through aseismic creep (either constant or periodic) or much smaller in the presence of locked zones along the plate boundary. Knowledge of the amount and distribution of locking on subduction faults is essential for improving our understanding on the hazard they pose, given that it has been demonstrated that the spatial extent of large earthquake ruptures sometimes correlates well with the higher locking regions of the subduction faults (Chlieh et al., 2011; Konca et al., 2008; Loveless & Meade, 2011; Moreno et al., 2010; Nocquet et al., 2017; Protti et al., 2014).

Although the pattern of interseismic locking on the majority of subduction zones has been mapped in detail and at some of them it has been repeatedly revisited, the Hellenic subduction system remains largely unstudied and unconstrained with regard to the spatial accumulation of elastic strain. In this context, only a few studies have exclusively examined the degree of locking of the Hellenic subduction system using geodetic data, which comprise the main type of observations for constraining locking models. Additionally, even among these studies, contradictory conclusions have been reached. Reilinger et al. (2010) and Vernant et al. (2014) gave evidence for a predominantly aseismic behavior of the Hellenic subduction, while Ganas and Parsons (2009) concluded that the interface is almost fully locked. There are still open questions related to the interseismic strain accumulation across the Hellenic subduction system. Are there regions of the plate interface that are stuck, indicating greater potential for larger earthquakes? What fraction of the Nubia/Eurasia convergence rate is accommodated by the subduction interface and what fraction is accommodated by the high-angle splay thrusts which branch off the interface (Mouslopoulou et al., 2015, 2025; Shaw et al., 2008)? In this paper, which is a companion to Chousianitis et al. (2026), we investigate the degree of interseismic locking along the Hellenic subduction system using a kinematic block model constrained by GPS velocities and earthquake slip vectors. With the block modeling approach we represent the present-day active deformation across the Aegean region as a combination of block rotations and elastic locking on the block-bounding faults, including the Hellenic subduction system. In the companion paper (Chousianitis et al., 2026), we describe the setup of the block model and presente the results referring to the upper plate structures, while in this paper we focus on the Hellenic subduction system. We explore the details of spatially variable locking along the plate interface and the Hellenic and Ptolemy trough splay faults and provide constraints on the distribution and rates of slip deficit accumulation. Our elastic-kinematic block model which is presented in its entirety in this and its companion paper, facilitates quantification of the deformation of the entire Aegean region, in which the contribution of subduction and upper plate faulting have been simultaneously taken into account.

2. Overview of the Hellenic Subduction System

The broader region of Greece is located in eastern Mediterranean, a geodynamically complex area where three tectonic plates meet and interact together. The key-structure of this setting is the Hellenic Arc, a subduction zone system where the remaining quasi-oceanic lithosphere subducts under the Aegean Sea due to the convergence between the Eurasian and the Nubian continental plates. The 80 Myr-evolution of the Hellenic Arc starts with the subduction front placed much farther north from its current position, where Thrace lies today (Ring et al., 2010; Jolivet et al., 2013, and references therein). A southward migration, due to the roll-back and retreat of the subducting oceanic slab, brings the Hellenic Arc to its present position (e.g., Faccenna et al., 2003; Jolivet & Brun, 2010; Jolivet et al., 2013; Le Pichon & Angelier, 1981; Menant et al., 2016; Taymaz et al., 1991). To the north of the present-day subduction deformation front we successively see the Mediterranean Ridge accretionary complex, the Mediterranean Ridge backstop which comprises the northern boundary of the accretionary complex, and the trough (aka "trench") system of the Hellenic Arc which is located in the forearc region and consists of the Hellenic Trough (aka Hellenic Trench) at its western part and the en echelon Strabo, Pliny and Ptolemy troughs at its eastern part (Figure 1). Here we note that the term trench which is often used to describe these features of the Hellenic subduction system does not correspond to the typical oceanic trench which is found at other subduction environments, but has become part of the nomenclature to describe these deep bathymetric escarpments in the forearc region that inherently represent oceanic troughs.

The properties and dynamics of the subducting Eastern Mediterranean quasi-oceanic remaining lithospheric slab under the Aegean has been a focus of interest for many geoscientists. Preliminary investigations during the late 1980s grossly defined the slab's geometry, while subsequent studies proposed refined 3D models (Bohnhoff et al., 2001; Chang et al., 2010; Endrun et al., 2004; Gesret et al., 2011; Hatzfeld, 1994; Meier et al., 2007; Papazachos et al., 2000; Piromallo & Morelli, 2003; Sodoudi et al., 2006; Spakman et al., 1988; Vaněk et al., 1987). Over the past two decades, the increased level of detail in these studies facilitated the identification of a down-dip tear on the eastern part of the Hellenic subduction zone (e.g., Bocchini et al., 2018; Jolivet et al., 2013) and the association of the transition from oceanic subduction to continental subduction and collision in the region of the CTFZ either with a trench-parallel tear (Wortel & Spakman, 2000), a trench-perpendicular tear (Suckale et al., 2009), or a continuous ramp-style transition without an evident break (Pearce et al., 2012). Slab rollback and

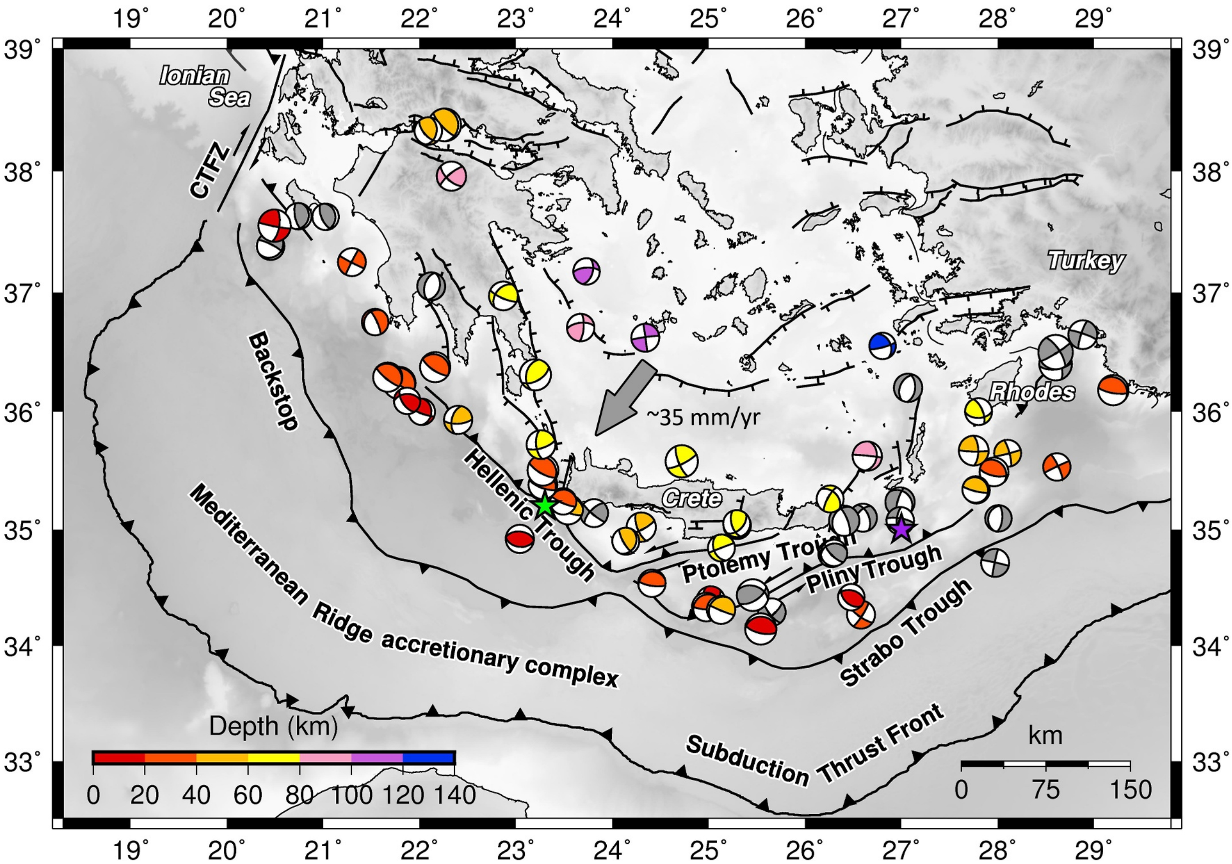

Figure 1. Seismotectonic setting of the broader region of southern Aegean. Bold gray arrow shows motion of the Aegean relative to the Eurasian plate. Focal mechanisms for earthquakes with $M_w \geq 5.5$ that occurred between 1965 and 2024 are from Shaw and Jackson (2010) and the moment tensor database of the National Observatory of Athens (https://bbnet.gein.noa.gr/HL/seismicity/mts). Events associated either with the subduction interface or with the downgoing slab are color coded by depth, while upper plate events are shown in gray color. Green and purple stars indicate the locations of the 365 AD and 1303 AD historical earthquakes, respectively. CTFZ: Cephalonia Transform Fault Zone.

fast trench retreat have been invoked to explain the strong along-strike curvature of the Hellenic subduction zone and the associated increased convergence obliquity toward its eastern part (Faccenna et al., 2004; Meier et al., 2007; Royden, 1993; ten Veen & Kleinspehn, 2003), and the rapid extension in the back-arc (Le Pichon & Angelier, 1979; McKenzie, 1978). The Hellenic Arc's curvature is generally well reflected at the seafloor morphology along the trough (aka "trench") system, where compression accommodated by thrust-faulting earthquakes is associated with the Hellenic Trough to the west, while a more complex regime which is characterized by local transpression, or even transtension, is expressed along the en echelon Ptolemy, Pliny and Strabo troughs (Bohnhoff et al., 2005; Le Pichon & Angelier, 1979; Mascle et al., 1986; Özbakir et al., 2013).

Seismicity related to the Hellenic subduction zone occurs as low-angle thrust events along the subduction interface, as intraslab events which are consistent with along-strike shortening and downdip stretching of the descending slab, and as shallower high-angle thrust earthquakes which are generated on splay faults in the overriding Aegean lithosphere (Benetatos et al., 2004; Meier et al., 2007; Shaw & Jackson, 2010; Taymaz et al., 1990). According to the latest studies, such splay thrusts which branch upward from the subduction interface and are located south of Crete across the trough (aka "trench") system of the Hellenic Arc, can potentially host rare great earthquakes (Howell et al., 2015; Mouslopoulou et al., 2015; Shaw & Jackson, 2010). A prime example is the 365 AD M_w 8.3–8.5 Crete earthquake which has been attributed to an upper plate splay fault consistent with the Hellenic Trough (Shaw et al., 2008), although an entirely different faulting mechanism is proposed by Ott et al. (2021) who suggested normal faulting. Toward the south, seismicity extends up to the Mediterranean Ridge backstop which marks the inner limit of the Mediterranean Ridge, whereas the accretionary complex shows extremely rare seismic activity (Le Pichon et al., 2002; Meier et al., 2004; Shaw & Jackson, 2010; Taymaz et al., 1990).

Despite the important role of the Hellenic subduction system in the geodynamic processes of Eastern Mediterranean, the way that the rapid Nubia/Eurasia convergence rate (~35 mm/yr) is accommodated across this plate boundary zone remains only loosely constrained and even controversial. Jackson and McKenzie (1988), using earthquake data, proposed that most of the Nubia/Eurasia relative convergence occurs aseismically, with subduction earthquakes accommodating only a small fraction of the convergent motion. Updated seismicity data used by Shaw and Jackson (2010) confirmed the dominantly (~80%) aseismic behavior of the Hellenic subduction system and proposed that seismic slip occurring on the subduction interface, as well as on large splay thrust faults, absorbs the remainder (~20%) of the total convergence rate. The majority of geodetic studies also point to a low level of locking at the Hellenic subduction system. In this context, the models used in Reilinger et al. (2010) and Vernant et al. (2014) satisfied the GPS data when interseismic locking on the subduction interface and the Hellenic Trough was less than ~0.15. We note, however, that these studies did not attempt to estimate spatially variable locking distributions, but the modeling was performed on the assumption of uniform coupling. In a more recent study, Saltogianni et al. (2020), using GPS velocities from stations located solely onshore Crete and Gavdos, calculated spatially variable slip rate deficits for the part of the Hellenic subduction system to the south of Crete. They concurred with the previous studies on the principally aseismic accommodation of convergence, yet they resolved two locations within the Hellenic subduction system exhibiting stronger locking. These more strongly locked regions are situated offshore western Crete and beneath central-eastern Crete and their average slip rate deficits induce locking which is not greater than 20%. However, Floyd et al. (2023), on the basis of GPS velocity profiles, identified strong coupling only around western Crete, with coupling values as high as 40%. Contrary to all aforementioned studies which support weak locking of the Hellenic subduction system, Ganas and Parsons (2009) used a finite element model to simulate the subduction of the Nubian plate under the Aegean plate and came to the conclusion of a nearly fully coupled interface. From all of the above, it becomes evident that the locking pattern of the Hellenic subduction system and its implications on the accommodation of the Nubia/Eurasia convergence needs further quantification and examination.

3. Elastic Interseismic Loading Along the Hellenic Subduction System

3.1. Data and Modeling Method

We assess the distribution and rate of elastic strain accumulation along the Hellenic subduction system on the basis of the back-slip concept and the elastic half-space dislocation formulas of Okada (1992). The calculations were performed using the TDEFNODE inversion code (McCaffrey, 2009), and the data to constrain the models consisted of 832 GPS-derived horizontal velocities along with 146 slip vector azimuths (Figure 2). These GPS velocities were compiled by combining published solutions from Briole et al. (2021), Kurt et al. (2023), and Ergintav et al. (2023). The rotation of these data sets into a common Eurasian reference frame was achieved by estimating their angular velocities as part of the inversion, together with block kinematics and fault locking parameters, thereby ensuring kinematic consistency between the GPS velocity fields, the block motions and the fault models. The slip vector azimuths were extracted using solutions of the European-Mediterranean Regional Centroid Moment Tensor (RCMT) Catalog (Pondrelli, 2002). Further information on the GPS and earthquake slip vector data can be found in the companion article Chousianitis et al., 2026). The regional kinematic block model for the Aegean region that we developed to facilitate quantification of the present-day deformation, incorporates the joint effects of subduction zone dynamics and upper plate processes. In view of that, we invert the GPS and earthquake slip vector data as a combination of elastic lithospheric block rotations and locking on block-bounding faults. Locking reflects the amount at which the fault surface is not slipping; instead of moving with the expected long-term motion, the locked fault exhibits a slip deficit and accumulates elastic strain that can be potentially released through earthquakes. The level of locking is associated with the scalar coupling coefficient ϕ which is zero ($\phi = 0$) when the fault is freely slipping and one ($\phi = 1$) when the fault is fully locked. In the block model, we defined the three-dimensional (3-D) geometry of the faults by means of nodes (specified by their longitude, latitude and depth coordinates) along their fault planes. At each of these nodes a slip vector V that describes the relative motion of the two adjacent blocks is estimated using their respective angular velocities, and back-slip is applied at a rate of ϕV to give the slip rate deficit vector. With TDEFNODE we inverted the GPS velocities and earthquake slip vectors to estimate angular velocities of crustal blocks and the degree of locking on the block-bounding faults. The latter include important upper plate faults of the Aegean region, the Hellenic subduction

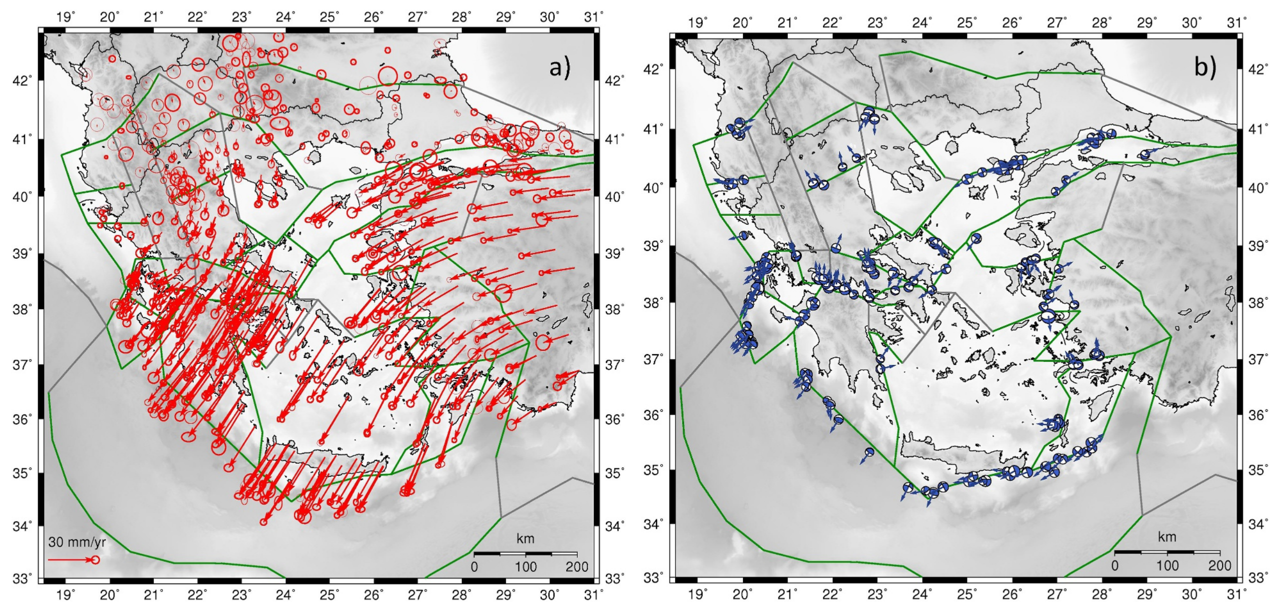

Figure 2. Data used in the inversions. (a) Horizontal GPS velocities and 95 percent confidence ellipses in the Eurasia reference frame defined in Chousianitis et al. (2026). (b) Earthquake focal mechanisms along with their corresponding slip vectors. Green and gray lines represent block-bounding active faults and free-slip block boundaries, respectively.

plate interface and the Hellenic and Ptolemy trough splay faults which branch upward from the interface and are considered components of the subduction system (Howell et al., 2015; Mouslopoulou et al., 2015; Shaw et al., 2008; Vernant et al., 2014). Details about the parameters of the upper plate faults of our block model are included in the companion article (Chousianitis et al., 2026). With regards to the Hellenic subduction system, using the model proposed by Bocchini et al. (2018) we approximated the geometry of the interface by nodes that form 14 downdip profiles with a spacing of 100 km in the along strike direction. The Hellenic and Ptolemy trough faults were set to dip 40° to the north with their planes intersecting the subduction interface at a depth of 40 km. Specific details on how we arrived at the preferred block model are given in the companion article (Chousianitis et al., 2026), where we discuss the modeling methodology and present a series of inversions with alternative block geometries and fault locking parameterizations. All inversions presented in Chousianitis et al. (2026) solved for a uniform coupling coefficient value ϕ at the upper plate faults and the Hellenic subduction system (i.e., the interface and the Hellenic and Ptolemy splays) and the obtained results in all cases shared a common feature; that is the estimation of low locking at the Hellenic subduction system with coupling coefficients ϕ ranging between 0 and 0.2. Hence, the low locking that our data suggest for the subduction interface and its two major splays appears to be a robust feature of the Hellenic subduction system given that this result is insensitive to alternative block model configurations. However, these low values of ϕ, which imply that the plate convergence is accommodated primarily through aseismic slip, were determined assuming uniform coupling across the entire surface area of each structure. Nonetheless, even though our modeling confirms a predominantly aseismic subduction, as suggested by Jackson and McKenzie (1988) and Shaw and Jackson (2010) using seismic data and Reilinger et al. (2010) and Vernant et al. (2014) using geodetic data, along-strike and/or downdip variations in locking as well as existence of locked patches cannot be ruled out. Accordingly, after solving for uniform coupling coefficients across all block-bounding faults, we ran inversions where we solve for a uniform coupling coefficient value ϕ for each upper plate fault, but allow for variable locking on the Hellenic subduction zone interface and on the Hellenic and Ptolemy trough faults.

3.2. Resolution Tests

In order to evaluate the sensitivity of our data to the spatial distribution of interseismic coupling along the Hellenic subduction system, we performed a series of resolution tests that impose a synthetic locking distribution on the subduction interface, the Hellenic Trough splay fault and the Ptolemy Trough splay fault with its eastern continuation up to the area south of Rhodes. We initially constructed a forward fault locking distribution

10.1029/2025JB033219

employing a checkerboard-style pattern (Figures 3a and 3e). After generating synthetic velocities and slip vectors from this forward model, we added random noise to the observations using the standard deviations of the real data and an inverse solution is estimated to see how well the imposed locking distribution was re-created (Figures 3b and 3f). Additionally, to examine how initial conditions influence the results, we performed a second checkerboard test, where we reversed the initial coupling coefficient values of the rectangular fault patches with respect to the first test, while keeping all other parameters the same (Figures 3c and 3g).

The results of the resolution tests indicate that station distribution is crucial for resolving variations in locking along the interface. Distance from GPS stations appears to be the primary controlling factor, consistent with the fundamental properties of Green's functions that describe how ground deformation signals diminish with increasing source-to-site distance. Fault depth also significantly influences the inversion results. Deeper patches converge more reliably to the coupling values of the starting model compared to the up-dip part of the interface. Specifically, while locking down to 5 km cannot be resolved and resolution down to 10 km remains low, the ability of the current data to resolve variations in locking below 10 km is good, as evidenced by the small discrepancy between the initial checkerboard locking distributions (Figures 3a and 3c) and the reproduced ones (Figures 3b and 3d). The imposed locking patterns on the splay faults of the subduction system (Figures 3e and 3g), are also successfully recovered (Figures 3f and 3h), demonstrating that the available data provide sufficient sensitivity to resolve first-order variations in locking on these structures. Overall, the resolution tests confirm that the chosen discretization in both strike and dip directions is appropriate for detecting the essential characteristics of the locking distribution on the Hellenic subduction system.

3.3. Best Fitting Model

We parameterize the interseismic locking distribution on the Hellenic subduction plate interface and the Hellenic and Ptolemy trough faults in two ways. In the first parameterization type, called the constrained model, we impose complete locking at the surface ($\phi = 1$ at $z = 0$) and treat the deeper fault nodes as independent of each other, with the only constraint being the downdip decrease of the coupling coefficient. In the second type, called the unconstrained model, we let the surface nodes vary freely and remove the downdip constraint, thus allowing for completely independent node values in both strike and depth. The most important difference between these two parameterizations is that with the first, locking extends to the subduction thrust front while with the second, locking extends to the surface only if the data require it. For these inversions we use the block geometry of the best fit model which is depicted in Figure 8 of the companion article (Chousianitis et al., 2026) and apart from the three structures of the Hellenic subduction system where we allow spatially variable locking, all other faults are treated as in the best fit model of the companion article, that is assuming uniform coupling throughout their surface. Because in all "variable locking" inversions we increased the number of free parameters due to the additional coupling coefficients, we fixed the ϕ values of all other faults to their initial estimates shown in Figure 10a of the companion article (Chousianitis et al., 2026) to balance as much as possible the degrees of freedom and avoid an underdetermined problem.

The unconstrained inversion, where we allowed ϕ values to vary both along-strike and downdip, resulted in a lower reduced chi-squared misfit ($X_n^2 = 5.021$) compared to the constrained inversion ($X_n^2 = 6.276$) and a better fit to the GPS velocities (normalized RMS 1.826 vs. 2.207) and the slip vectors (normalized RMS 2.003 vs. 3.568). The variance was also reduced and the F-ratio test confirms that the improvement in fit achieved with the unconstrained model is statistically significant at the 99% level because the calculated F value (21.996) is much greater than the $F_{0.01}$ critical value (1.916). Accordingly, the unconstrained locking model represents our best fit model for the Hellenic subduction system. Furthermore, GPS velocity residual maps (Figure S1 in Supporting Information S1) show that residuals in the central and southern Aegean, particularly across Crete, are noticeably larger in the constrained compared to the unconstrained inversion, implying that allowing ϕ to vary freely provides a locking distribution across the Hellenic subduction system that reproduces more accurately the observed deformation field. The corresponding histograms of the GPS velocity residuals (Figure S2 in Supporting Information S1) similarly show a narrower and more symmetric distribution for unconstrained locking model, with fewer extreme values and a mean closer to zero, indicating a reduction in both bias and scatter relative to the model where ϕ values were forced to be 1 at the surface and decrease downdip.

10.1029/2025JB033219

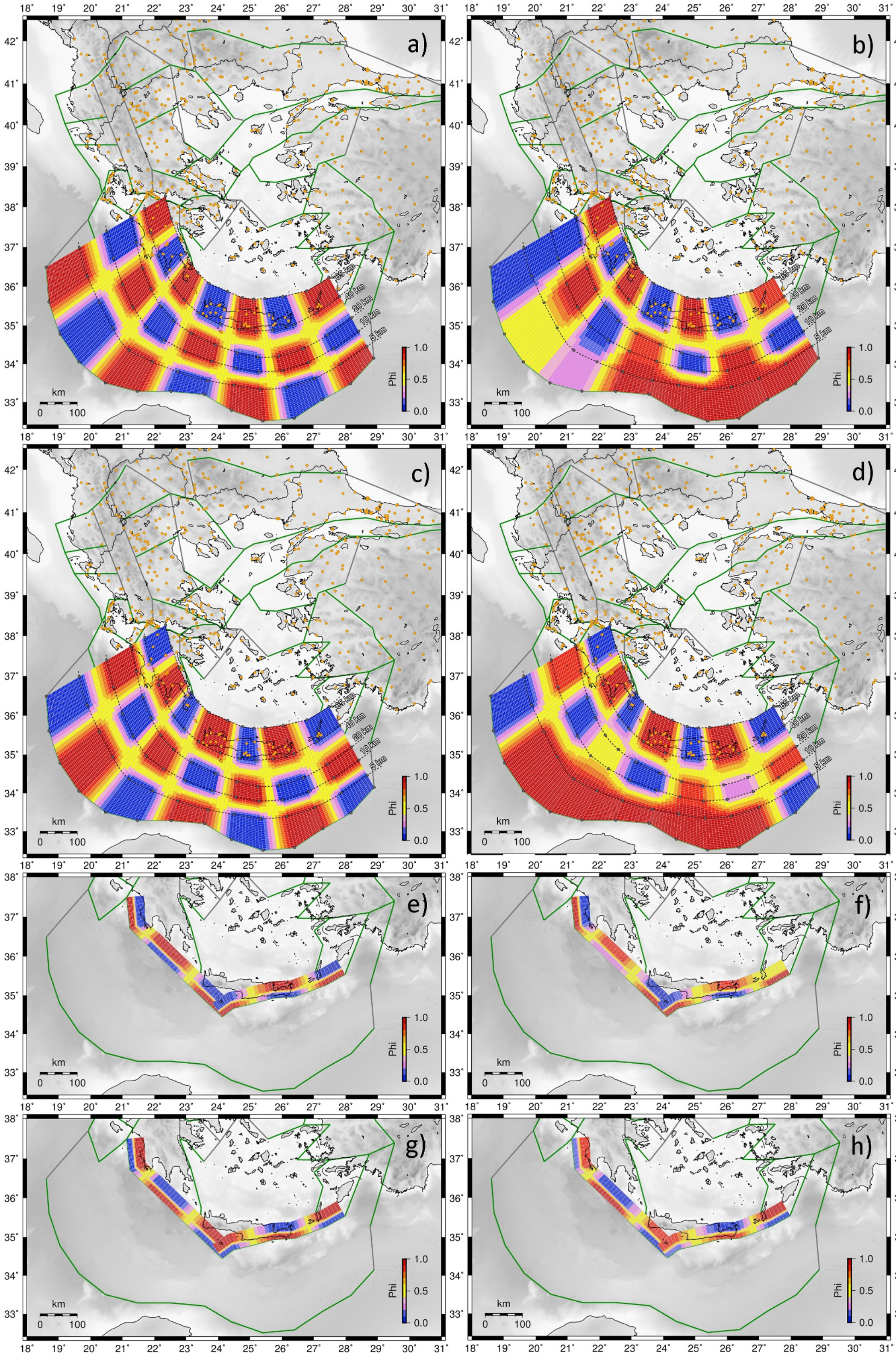

Figure 3.

3.4. Slip Rates Along the Hellenic Subduction System

Our kinematic model predicts a megathrust convergence rate which gradually increases from 18.7 ± 1.2 mm/yr in the east to 22.6 ± 0.6 mm/yr in the west (Figure 4). The convergence direction from longitude 20°E to 26.5°E is nearly normal to the margin and hence, it is primarily accommodated by dip-slip motion. West of 20°E and east of 26.5°E, however, the subduction direction becomes oblique to the thrust front and the model resolves both margin-normal (i.e., contractional) and margin-parallel (i.e., strike-slip) components. Moreover, these margin-parallel components demonstrate that the western and eastern parts of the subduction interface are characterized by an opposite sense of lateral motion, accommodating dextral and sinistral shear, respectively.

Estimated slip rates for the NW-SE trending Hellenic Trough splay fault indicate nearly pure compressional motion of 16.4 ± 0.7 mm/yr, in accordance to the prevalence of reverse-faulting focal mechanisms in that region (Benetatos et al., 2004; Shaw & Jackson, 2010). Farther east, the ENE-WSW trending Ptolemy Trough splay fault accommodates on average 15.3 ± 0.9 mm/yr of oblique (left-lateral) shortening (Figure 4). This oblique sense of slip is compatible with the observed thrust and sinistral strike-slip faulting earthquakes in that area, whose slip vectors are oriented roughly parallel to the subduction direction (i.e., ∼SW) in the case of the thrust events and roughly parallel to the strike of the steep escarpments associated with the trough (aka “trench”) system of the forearc (i.e., ∼WSW) in the case of the strike-slip events (Shaw & Jackson, 2010).

The eastern continuation of the Ptolemy Trough fault, extending from the offshore region south of Karpathos to south of Rhodes, also accommodates a combination of strike-slip and contraction, but here the contractional motion dominates. The direction of the relative motion vector across this boundary exhibits an eastward rotation relative to that across the Ptolemy Trough, becoming southward-directed with an average rate of 19.3 ± 1.0 mm/yr. We also note that further to the NE, our results for the NW-dipping Rhodes Basin Fault support a sinistral transpressional regime, with rates on the order of 18.6 ± 1.2 mm/yr, where the majority of the deformation is accommodated by horizontal shear rather than vertical shortening (Chousianitis et al., 2026).

Finally, it is worth noting that the estimated slip rates, ranging from 18.7 to 22.6 mm/yr for the subduction interface and on average from 15.3 mm/yr for the Ptolemy Trough splay fault to 16.4 mm/yr for the Hellenic Trough splay fault and 19.3 mm/yr for the eastern continuation of the Ptolemy Trough splay fault up to the area south of Rhodes, add up to ∼35 mm/yr; that is they jointly give the present-day convergence rate between the Aegean and Nubian plates. Given these rates, it is deduced that approximately 60% of the overall Aegean-Nubia relative plate motion is accommodated on the plate interface and 40% on the major splay faults of the subduction system. To evaluate the robustness of this partitioning, we performed additional inversions in which slip rates on the splay faults were constrained to lower and higher values and the model was recomputed (Figure S3 in Supporting Information S1). Imposing substantially lower slip rates (5–6 mm/yr) resulted in a significantly poorer fit compared to the best fit model (reduced chi-squared misfit increasing from $X_n^2 = 5.021$ in the best fit model to $X_n^2 = 6.292$), with the inversion compensating for the imposed low splay-fault slip by increasing slip rates on the plate interface to 27–32 mm/yr. Conversely, forcing high splay-fault slip rates (>25 mm/yr) also degraded the fit ($X_n^2 = 5.576$), with the inversion reducing slip rates on the plate interface to 10–15 mm/yr. Intermediate tests, where we imposed slip rates on the splay faults to values of 10–11 mm/yr and 20–25 mm/yr yielded misfits larger than that of the preferred solution as well ($X_n^2 = 5.548$ and 5.198, respectively, compared to $X_n^2 = 5.021$ of the best fit model). Taken together, these tests suggest that the comparable slip rates inferred for the subduction interface (∼19–23 mm/yr) and the splay faults (∼15–19 mm/yr) in the preferred solution are required by the data and indicate that end-member scenarios, where most convergence is accommodated either on the plate interface or on the splay faults, are inconsistent with the observations.

3.5. Locking Model of the Hellenic Subduction System

Our preferred model suggests that the eastern half of the subduction interface is fully creeping, in contrast to the western half, which displays spatially variable coupling with ϕ values that ranged from zero to 0.4 (Figure 5a). In

Figure 3. Checkerboard tests for locking along the Hellenic subduction system. (a–d) Results for the plate interface. (e–h) Results for the splay faults. (a, e) Forward fault locking distributions. (b, f) Solutions obtained from inversion of synthetic data generated by the model illustrated in (a) and (e). (c, g) Same as (a) and (e) but with reversed initial coupling coefficient values. (d, h) Solutions obtained from inversion of synthetic data generated by the model illustrated in (c) and (g). Green and gray lines represent block-bounding faults and free-slip boundaries of the elastic block model, respectively. Locations of GPS sites are shown as orange circles. Dashed lines and gray circles indicate contours and nodes along the plate interface, respectively.

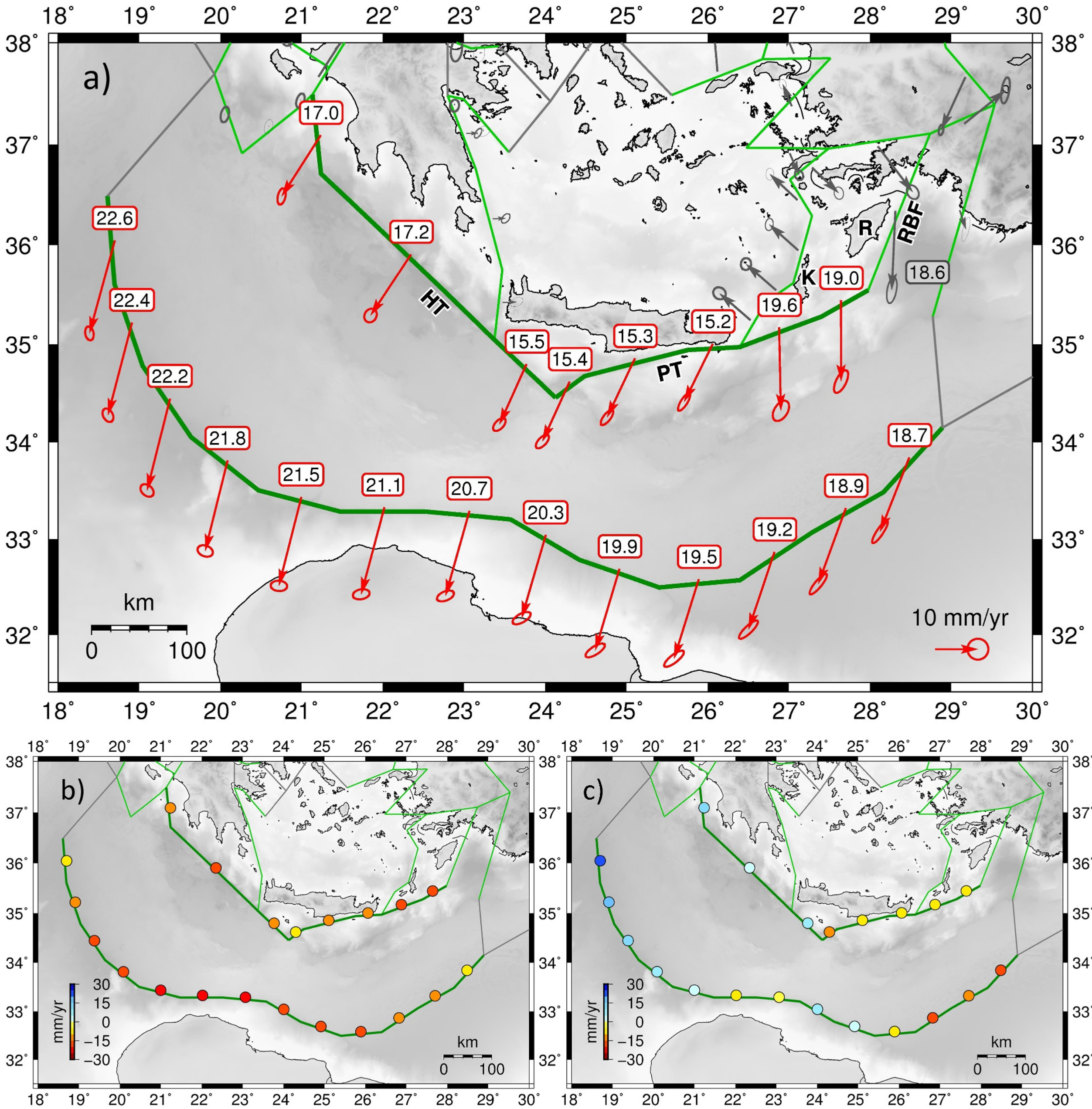

Figure 4. (a) Predicted relative slip vectors (in red) across the boundaries of the elastic block model with their 95% confidence ellipses. They depict the movement of the hanging wall relative to the footwall. Numbers indicate the total velocity magnitude in mm/yr corresponding to each vector. Green and gray lines outline the block model geometry, indicating boundaries along which backslip is applied and those that are free-slipping, respectively. Thicker green lines denote boundaries related to the Hellenic subduction system where we imposed spatially variable locking and which are discussed in this paper, while narrower lines represent upper plate boundaries with their relative slip vectors (in gray) which are discussed in the companion article (Chousianitis et al., 2026). (b) Fault-normal and (c) fault-parallel components of the relative slip vectors. Positive values correspond to divergence and right-lateral shear. HT: Hellenic Trough; PT: Ptolemy Trough; K: Karpathos; R: Rhodes; RBF: Rhodes Basin Fault.

all models, the locking is confined in the offshore area to the SW of Kythira island and western Crete as well as beneath SW Peloponnese. These moderately locked patches extend from 10 to 50 km depth, where the resolution of our model is robust, as demonstrated by the checkerboard tests (Figure 3). Our result also suggests that the up-dip part of the interface, which extends from the subduction thrust front down to 10 km depth, is freely slipping. Although we acknowledge that the resolution in this shallowest section of the interface is poor, we note that this outcome appears consistent with a) the very low level of seismicity in the accretionary complex which suggests that it deforms aseismically, and b) the very low angle of the slab dip in the first 10 km which imply low

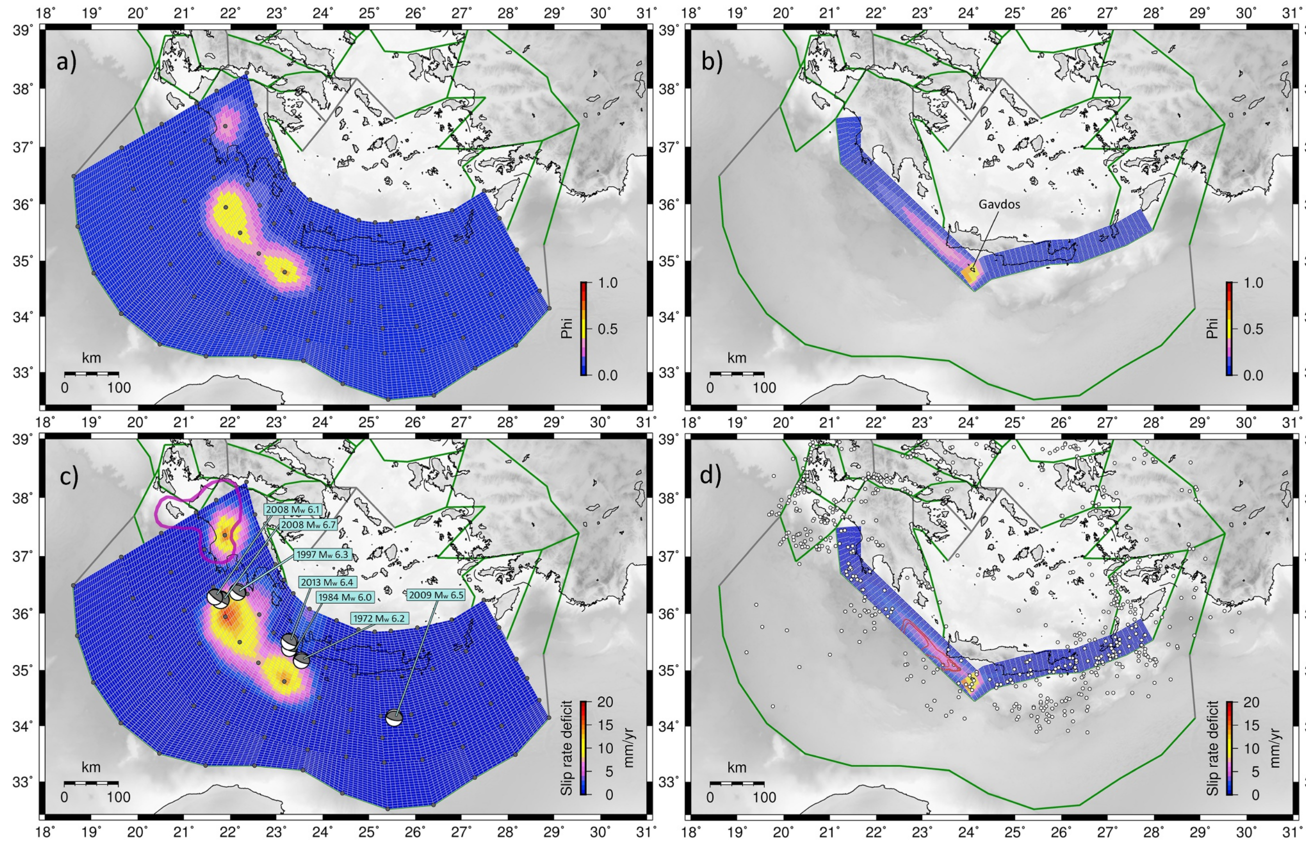

Figure 5. Locking model of the Hellenic subduction zone interface and the Hellenic and Ptolemy trough faults. (a, b) Locking fraction (ϕ values). (c, d) Slip rate deficit magnitudes. Results for the Hellenic subduction zone interface are shown in (a, c), and for the Hellenic and Ptolemy trough faults in (b, d). Focal mechanisms of the largest interplate earthquakes that occurred after 1965 in the subduction interface are from Shaw and Jackson (2010) and the moment tensor database of the National Observatory of Athens (https://bbnet.gein.noa.gr/HL/seismicity/mts). The extent of the slow-slip event in 2018 is outlined with a purple line (after Saltogianni et al., 2021). The coseismic slip of the 365 AD Crete earthquake is illustrated with a red line (after Mouslopoulou et al., 2015). Earthquakes with $M \geq 4.5$ since 1980 from the declustered catalog of Chousianitis et al. (2024) are also shown.

shear stress on the décollement beneath the accretionary complex, favoring free slip along the interface. Free slip is also supported by the presence of Messinian evaporites along the décollement, whose low permeability leads to high fluid pressures that reduce effective stress, thereby contributing to the reduced seismic activity.

The slip rate deficit across the interface is illustrated in Figure 5c. It is a quantity of interest in the context of seismic hazard because it is associated with the accumulation of elastic strain that can be released during earthquakes, and equals the product ϕV, of the coupling coefficient ϕ with the relative slip velocity V along the fault surface. The three patches of moderate coupling that our preferred model reveals across the western downdip section of the subduction interface, exhibit average slip rate deficits of 8 mm/yr, 10 mm/yr and 6 mm/yr on the southernmost, central and northernmost asperity beneath SW Peloponnese, respectively. These deficit rates, accumulated on the plate interface across an area of ∼380 km along-strike and ∼40 km downdip, account for 17%–28% of the long-term plate convergence rate (∼35 mm/yr) between the Aegean and Nubian plates. The estimated slip rate deficit can be used to assess the rate of moment accumulation across a locked asperity, which reflects the build-up of elastic strain energy (i.e., moment) that could be released through seismic slip during future earthquakes. To this end, we apply the equation $\dot{M}_0 = \mu \sum S_d A$, where μ is the shear modulus (assumed to be 30 GPa), S_d is the slip rate deficit and A is the area of each fault sub-segment, and estimate a moment accumulation rate of 5.85×10^{17} N·m/yr, 9.12×10^{17} N·m/yr and 4.13×10^{17} N·m/yr for the northernmost asperity beneath SW Peloponnese, the central asperity to the SW of Kythira island and the southernmost asperity to the SW of western Crete, respectively. These amounts of moment are equivalent to an M_w 5.8, an M_w 5.9 and an M_w 5.7 earthquake per year, respectively, for the aforementioned asperities or larger events on longer timescales. We note that since our locking model represents the steady accumulation of strain during the seismic cycle, these

10.1029/2025JB033219

rates do not account for the moment released by possible transient events that could contribute to the overall deformation budget. However, current knowledge indicates that the Hellenic subduction system does not exhibit noteworthy time-dependent transient deformation components. So far, only one such case has been documented in the literature (Briole et al., 2021; Mouslopoulou et al., 2020), involving a transient signal that preceded the 2018 M_w 6.8 Zakynthos earthquake (Chousianitis & Konca, 2019; Papadimitriou et al., 2021). This possible slow-slip event occurred beneath Zakynthos and western Peloponnese at depths between 20 and 50 km, although estimates of the released moment differ, with Mouslopoulou et al. (2020) estimating a moment equivalent to M_w ~6.3, whereas Briole et al. (2021) reported a lower estimate of M_w ~5.8. This scarcity of documented transients in the Hellenic subduction system can be attributed to both insufficient instrumental coverage–particularly due to the offshore location of much of the subduction interface which makes the detection of small transients difficult or impossible–and the inherently low occurrence of larger transient events along the plate boundary.

Regarding the upper plate splay faults, our model results display a pattern analogous to that of the subduction interface. In this context, the eastern structure, that is the Ptolemy Trough splay fault with its eastern continuation up to the area south of Rhodes, appears to be uncoupled. The western structure on the other hand, that is the Hellenic Trough, displays low degrees of coupling ($\phi < 0.3$) across a broad region extending from its southeastern termination offshore of Gavdos island to offshore south-central Peloponnese (Figure 5b). We note here that offshore of Gavdos island, our model resolved a small, moderately coupled asperity ($\phi < 0.6$) located at the southwesternmost termination of the Ptolemy Trough fault. This small asperity, due to its location, overlaps with the low coupled section of the Hellenic Trough fault, so we cannot be certain whether this ~30 km × 30 km asperity is indeed situated on the Ptolemy Trough fault or on the Hellenic Trough fault. However, what can be implied with confidence is that the region offshore of Gavdos island exhibits higher degrees of coupling compared to the rest of the low coupled section of the Hellenic Trough fault. In terms of deficits, our model predicts an average slip rate deficit of 4.5 mm/yr across the Hellenic Trough fault (its distribution is depicted in Figure 5d) and a corresponding moment deficit accumulation rate of 5.9×10^{17} N·m/yr. If a single event like the 365 AD Crete earthquake (M_w 8.3–8.5) were to release the entire slip deficit, the recurrence time would be ~5,400 years if this event had a magnitude of M_w 8.3, and ~10,700 years if it had a magnitude of M_w 8.5.

To evaluate the sensitivity of the preferred unconstrained solution to uncertainties in the dip of the splay faults, we performed an inversion using alternative end-member dip values. To this end, and based on available seismicity data (Benetatos et al., 2004; Howell et al., 2015; Shaw & Jackson, 2010), we used a dip value of 25° for the western splay fault and 60° for the eastern splay fault and recomputed the locking distribution across the Hellenic subduction system. This test was designed to assess whether the inferred locking distribution of the best fit model is robust to plausible variations in fault dip of the splay thrust faults. The resulting coupling patterns on both the plate interface and the two splay faults are very similar to those of the preferred model, with only minor differences in the estimated coupling coefficients and slip-rate deficits and no significant change in the overall spatial pattern (Figure S4 in Supporting Information S1). Also, the reduced chi-squared misfit ($X_n^2 = 5.195$) of this run is slightly higher than that of the preferred solution. The result of this test indicates that the principal features of the locking distribution across the Hellenic subduction system are primarily controlled by the inverted data and plausible variations in splay-fault dip have only a limited influence on the overall coupling pattern.

4. Discussion

Though GPS data have been used to refine our understanding of the complex deformation patterns in the Aegean region for the past 35 years, few studies have specifically investigated the distribution and degree of kinematic coupling along the Hellenic subduction system. Furthermore, the Hellenic Arc displays along-strike heterogeneity in slab dip, convergence rate and upper plate deformation, while the occurrence of historical (e.g., the 365 AD M_w 8.3–8.5 earthquake offshore western Crete; see Figure 5d) and recent large subduction earthquakes (e.g., the 2008 M_w 6.7 Methoni earthquake, the 2009 M_w 6.5 earthquake offshore south of central Crete, and the 2013 M_w 6.4 earthquake offshore western Crete; see Figure 5c), although rare, strongly suggest the presence of locked and/or partially locked segments along the Hellenic subduction system. The spatially variable locking solution obtained from our kinematic block modeling confirms the primarily aseismic accommodation of the Aegean-Nubia convergence, as suggested by most previous studies (e.g., Jackson & McKenzie, 1988; Vernant et al., 2014), but also identifies low-moderately locked (up to 40%) patches that accumulate interseismic slip deficit and may represent potential sites for future seismic release. These patches are located in the western part of the subduction interface and along the Hellenic Trough splay fault, highlighting a contrast with the eastern Hellenic subduction

10.1029/2025JB033219

system (i.e., the eastern subduction interface and the Ptolemy Trough splay fault), which appears to be completely uncoupled. It should be noted here that, even though convergence may be entirely accommodated by aseismic slip, moderate earthquakes of M_w ~5.0–6.0 (or even larger) can still occur under suitable mechanical and frictional conditions (Bürgmann, 2018; Kaneko & Lapusta, 2008; Noda & Lapusta, 2013).

Our new locking estimates in the western part of the Hellenic subduction system indicate that the locked portion of the interface extends from beneath the southwestern Peloponnese to the offshore region southwest of western Crete, at depths ranging from 10 to 50 km, while along the Hellenic Trough fault it spans a broad region, from its southeastern termination offshore of Gavdos Island to offshore south-central Peloponnese. These sections represent potential slip areas for future earthquakes and although it is uncertain whether failure will occur as one large rupture or as multiple smaller events, they have implications for the buildup of elastic strain and therefore present seismic and tsunami hazard. Regarding the subduction interface, and considering that the prevailing view is that the 365 AD and the 1303 AD earthquakes ruptured splay thrusts within the Hellenic forearc rather than the interface itself (Howell et al., 2015; Mouslopoulou et al., 2015; Shaw et al., 2008), the notable rarity of great earthquakes ($M \geq 8.0$) suggests that the three coupled asperities identified in our locking model might not represent coherent locked patches in the conventional sense (i.e., which rupture almost completely during a great megathrust earthquake, as seen in Chile, Alaska and Japan). Instead, they likely consist of many smaller velocity-weakening asperities embedded in a generally creeping (velocity-strengthening) background (Hetland & Simons, 2010), which although capable of rupturing, are too small to grow into great earthquakes. The situation along the Hellenic Trough fault within the forearc, however, may differ, as modeling and paleoseismic evidence indicate that it hosted the 365 AD earthquake; hence it can be considered capable of producing events of similar magnitude (Shaw et al., 2008; Shaw & Jackson, 2010). If this interpretation is correct, it suggests that the broad, partially locked asperity (0%–30%) along the Hellenic Trough fault can be interpreted as a region of velocity-weakening behavior, prone to generating great and potentially tsunamigenic earthquakes, as it is much steeper than the subduction interface, similar to the 365 AD event. However, given the debate about this event (Ott et al., 2021; Shaw et al., 2008), as well as the inherent uncertainty in assessing the size, location and rupture characteristics of historical earthquakes, it cannot be excluded that the accumulated elastic strain might not be released in a single massive 365 AD-type earthquake, but rather gradually through a sequence of more frequent, moderate-magnitude events.

The spatial distribution of interseismic coupling along the subduction interface is examined in relation to past ruptures and the slow aseismic slip that preceded the 2018 Zakynthos earthquake. It appears that the locations of the largest interplate earthquakes which occurred after 1965 in the western part of the subduction interface are spatially correlated with the coupled regions of the inferred locking shown in Figure 5c. Specifically, the 2008 Methoni earthquake (M_w 6.7), which is the largest subduction thrust event of the instrumental period, as well as the 1997 earthquake (M_w 6.3), which occurred nearby and had a similar focal mechanism, cluster at the western edge of the central coupled patch. Similarly, the 1972 (M_w 6.2), the 1984 (M_w 6.0) and the 2013 (M_w 6.4) earthquakes which occurred a few kilometers SW of western Crete cluster downdip at the edge of the eastern coupled patch. These observations suggest that strong earthquakes in the western part of the subduction interface are closely associated with the observed locking pattern, with weakly locked patches guiding their spatial distribution and indicating the locations where future events are most likely to occur. During the instrumental period, the eastern part of the subduction interface was less active as regards strong earthquakes, with only the 2009 M_w 6.5 earthquake south of central Crete, exceeding M_w 6.0. In this context, and recalling that aseismic subduction does not preclude moderate or strong earthquakes when local stress, frictional properties, or fault heterogeneity favor seismic slip, the relatively higher occurrence of strong earthquakes along the western part of the interface appears consistent with our interseismic locking solution, suggesting a higher level of active strain accumulation there compared to the eastern part.

The third coupled patch, which is located beneath SW Peloponnese, is not associated with strong earthquakes but shows a spatial correlation with a transient aseismic slip detected beneath western Peloponnese at ~20–50 km depth along the plate interface (Saltogianni et al., 2021). The occurrence of this transient slow-slip event in the same area suggests that this patch accommodates strain primarily through episodic aseismic slip, that is the slip deficit is released in transient events rather than through seismic ruptures, which explains the absence of strong interface earthquakes beneath western Peloponnese. Compared with the eastern and central patches, which correlate with past seismic ruptures, the SW Peloponnese patch exhibits lower coupling, although all three patches are characterized by low to moderate coupling values. However, their different behavior highlights that

10.1029/2025JB033219

similar coupling values do not necessarily reflect similar mechanical states or slip modes. While the eastern and central patches have exhibited the release of accumulated strain through seismic ruptures, the SW Peloponnese patch appears to accommodate strain mainly through episodic aseismic slip, highlighting the spatial variability of slip behavior along the western part of the plate interface. These observations underline that low to moderate locking alone is not sufficient to distinguish slip modes and characterize seismic hazard, since patches with comparable locking can either generate strong earthquakes or release strain aseismically through transient slow-slip events, which further complicate hazard evaluation by being associated both with the inhibition of earthquake nucleation (Dascher-Cousineau & Bürgmann, 2024; Rolandone et al., 2018) and with the triggering of earthquakes and/or swarms (Brodsky & Lay, 2014; Cruz-Atienza et al., 2021; Moutote et al., 2023; Radiguet et al., 2016; Socquet et al., 2017). This finding for the western part of the Hellenic subduction interface may provide insights applicable to other weakly locked subduction margins such as in Costa Rica and Lesser Antilles/Puerto Rico (Kobayashi et al., 2014; Perry et al., 2025; Symithe et al., 2015).

Finally, with regard to the Hellenic Trough fault, the estimated locking distribution coincides well with the coseismic slip of the 365 AD Crete earthquake (Figure 5d). This spatial agreement, corroborated by the very low level of seismicity in this region, suggests that the partially locked asperity identified along this splay fault may represent a region of velocity-weakening behavior that accumulates strain and is capable of hosting great, potentially tsunamigenic earthquakes. This finding suggests that the Hellenic Trough splay fault can act as primary seismic source, capable of generating great 365 AD-type earthquakes even where the plate interface itself is weakly coupled or largely creeping. Of course, stress localization and variations in fault strength exert a fundamental control on the recurrence, timing, and rupture propagation (Scholz, 2019), but if similar events were to occur in the future, they could pose serious hazards to the eastern Mediterranean basin. These results underscore the need to explicitly account for forearc splay faults in regional seismic and tsunami hazard assessments, as their potential to generate great earthquakes challenges the conventional emphasis on the subduction interface alone.

5. Conclusions

We apply elastic block modeling, constrained by GPS velocities and earthquake slip vectors, to examine spatial variations in interseismic locking along the Hellenic subduction system. Our results indicate that although most of the plate motion is accommodated aseismically, the western section of the subduction interface hosts three coupled patches of low to moderate locking (0%–40%) at 10–50 km depth, whose slip rate deficits account for ∼15–30% of the total plate convergence. Two of these asperities, extending from offshore south Peloponnese to offshore southwest of western Crete, are spatially correlated with the locations of large interplate earthquakes while the third asperity, which is located beneath southwestern Peloponnese, coincides with a past transient slow-slip event. These findings underscore that slip behavior along the interface cannot be inferred solely from locking level, as patches with similar locking can result in either generating strong earthquakes or accommodating strain through episodic aseismic slip. A low-coupled area that spatially correlates with the coseismic slip of the 365 AD Crete earthquake was also identified along the Hellenic Trough splay fault, supporting the view that it is capable of hosting great, potentially tsunamigenic earthquakes. Finally, our data require higher degrees of locking on a confined region offshore of Gavdos island, which may lie on either the Hellenic Trough fault or the Ptolemy Trough fault. Contrary to the western part of the Hellenic subduction system which exhibits spatially variable locking, the kinematic block model suggests that the eastern part is completely uncoupled, highlighting a pronounced contrast between them. The results presented in this work demonstrate for the first time a link between large subduction-related earthquakes and the distribution of interseismic locking along the Hellenic subduction system. Although this connection appears particularly robust in the western part, occurrence of moderate or even larger earthquakes in the eastern uncoupled part cannot be ruled out under suitable mechanical and frictional conditions.

Conflict of Interest

The authors declare no conflicts of interest relevant to this study.

Availability Statement

The TDEFNODE control and input files that were used in this research and the final GPS velocity field are available at Chousianitis (2026). The computer code TDEFNODE that was used to model elastic lithospheric block rotations and locking on block-bounding faults is publicly available at McCaffrey (2023). Figures were made using GMT (Wessel et al., 2019), available at https://www.generic-mapping-tools.org.

Acknowledgments

We wish to thank the Editor, Anke Friedrich, for facilitating the simultaneous review process of this manuscript and its companion paper, and the Associate Editor for the efficient processing of our submission and valuable feedback. We also acknowledge the very thorough and constructive reviews of Andy Howell and an anonymous reviewer, which played a key role in strengthening this paper. The publication of this article in OA mode was financially supported by HEAL-Link.

References

Ambraseys, N. (2009). *Earthquakes in the mediterranean and Middle East: A multidisciplinary study of seismicity up to 1900* (p. 987). Cambridge University Press. https://doi.org/10.1017/CBO9781139195430

Benetatos, C., Kiratzi, A., Papazachos, C., & Karakaisis, G. (2004). Focal mechanisms of shallow and intermediate depth earthquakes along the Hellenic Arc. *Journal of Geodynamics*, *37*(2), 253–296. https://doi.org/10.1016/j.jog.2004.02.002

Biryol, C. B., Beck, S. L., Zandt, G., & Özacar, A. A. (2011). Segmented African lithosphere beneath the Anatolian region inferred from teleseismic P-wave tomography. *Geophysical Journal International*, *184*(3), 1037–1057. https://doi.org/10.1111/j.1365-246X.2010.04910.x

Bocchini, G. M., Brüstle, A., Becker, D., Meier, T., van Keken, P. E., Ruscić, M., et al. (2018). Tearing, segmentation, and backstepping of subduction in the Aegean: New insights from seismicity. *Tectonophysics*, *734*(735), 96–118. https://doi.org/10.1016/j.tecto.2018.04.002

Bock, Y., & Melgar, D. (2016). Physical applications of GPS geodesy: A review. *Reports on Progress in Physics*, *79*(10), 106801. https://doi.org/10.1088/0034-4885/79/10/106801

Bohnhoff, M., Harjes, H. P., & Meier, T. (2005). Deformation and stress regimes in the Hellenic subduction zone from focal mechanisms. *Journal of Seismology*, *9*(3), 341–366. https://doi.org/10.1007/s10950-005-8720-5

Bohnhoff, M., Makris, J., Papanikolaou, D., & Stavrakakis, G. (2001). Crustal investigation of the Hellenic subduction zone using wide aperture seismic data. *Tectonophysics*, *343*(3–4), 239–262. https://doi.org/10.1016/S0040-1951(01)00264-5

Briole, P., Ganas, A., Elias, P., & Dimitrov, D. (2021). The GPS velocity field of the Aegean. New observations, contribution of the earthquakes, crustal blocks model. *Geophysical Journal International*, *226*(1), 468–492. https://doi.org/10.1093/gji/ggab089

Brodsky, E. E., & Lay, T. (2014). Recognizing foreshocks from the 1 April 2014 Chile earthquake. *Science*, *344*(6185), 700–702. https://doi.org/10.1126/science.1255202

Brudzinski, M. R., & Allen, R. M. (2007). Segmentation in episodic tremor and slip all along cascadia. *Geology*, *35*(10), 907–910. https://doi.org/10.1130/G23740A.1

Brun, J. P., & Sokoutis, D. (2010). 45 m.y. of Aegean crust and mantle flow driven by trench retreat. *Geology*, *38*(9), 815–818. https://doi.org/10.1130/G30950.1

Bürgmann, R. (2018). The geophysics, geology and mechanics of slow fault slip. *Earth and Planetary Science Letters*, *495*, 112–134. https://doi.org/10.1016/j.epsl.2018.04.062

Bürgmann, R., Kogan, M. G., Steblov, G. M., Hilley, G., Levin, V. E., & Apel, E. (2005). Interseismic coupling and asperity distribution along the Kamchatka subduction zone. *Journal of Geophysical Research*, *110*(B7), B07405. https://doi.org/10.1029/2005JB003648

Chang, S. J., Van Der Lee, S., Flanagan, M. P., Bedle, H., Marone, F., Matzel, E. M., et al. (2010). Joint inversion for three-dimensional S velocity mantle structure along the Tethyan margin. *Journal of Geophysical Research*, *115*(B8), B08309. https://doi.org/10.1029/2009JB007204

Chlieh, M., Perfettini, H., Tavera, H., Avouac, J.-P., Remy, D., Nocquet, J.-M., et al. (2011). Interseismic coupling and seismic potential along the Central Andes subduction zone. *Journal of Geophysical Research*, *116*(B12), B12405. https://doi.org/10.1029/2010JB008166

Chousianitis, K. (2026). GPS velocities and earthquake slip vectors in the Aegean [Dataset]. *Zenodo*. https://doi.org/10.5281/zenodo.20268296

Chousianitis, K., & Konca, A. O. (2019). Intraslab deformation and rupture of the entire subducting crust during the 25 October 2018 Mw 6.8 Zakynthos earthquake. *Geophysical Research Letters*, *46*(24), 14358–14367. https://doi.org/10.1029/2019GL085845

Chousianitis, K., Sboras, S., Özbey, V., McCaffrey, R., & Ergintav, S. (2026). Block kinematics, interseismic coupling and fault slip rates in the Aegean region from GPS and earthquake slip vector data: 1. Upper plate structures. *Journal of Geophysical Research: Solid Earth*. *131*(7), e2025JB033218. https://doi.org/10.1029/2025JB033218

Chousianitis, K., Sboras, S., Mouslopoulou, V., Chouliaras, G., & Hristopulos, D. T. (2024). The upper crustal deformation field of Greece inferred from GPS data and its correlation with earthquake occurrence. *Journal of Geophysical Research: Solid Earth*, *129*(4), e2023JB028004. https://doi.org/10.1029/2023JB028004

Cosenza-Muralles, B., DeMets, C., Márquez-Azúa, B., Sánchez, O., Stock, J., Cabral-Cano, E., & McCaffrey, R. (2022). GPS-derived interseismic fault locking along the Jalisco–Colima segment of the Mexico subduction zone. *Geophysical Journal International*, *228*(3), 2174–2197. https://doi.org/10.1093/gji/ggab436

Cruz-Atienza, V. M., Tago, J., Villafuerte, C., Wei, M., Garza-Girón, R., Dominguez, L. A., et al. (2021). Short-term interaction between silent and devastating earthquakes in Mexico. *Nature Communications*, *12*(1), 2171. https://doi.org/10.1038/s41467-021-22326-6

Dascher-Cousineau, K., & Bürgmann, R. (2024). Global subduction slow slip events and associated earthquakes. *Science Advances*, *10*(35), eado2191. https://doi.org/10.1126/sciadv.ado2191

de Boorder, H., Spakman, W., White, S. H., & Wortel, M. J. R. (1998). Late Cenozoic mineralization, orogenic collapse and slab detachment in the European Alpine Belt. *Earth and Planetary Science Letters*, *164*(3), 569–575. https://doi.org/10.1016/S0012-821X(98)00247-7

Dragert, H., Wang, K. L., & James, T. S. (2001). A silent slip event on the deeper Cascadia subduction interface. *Science*, *292*(5521), 1525–1528. https://doi.org/10.1126/science.1060152

Elliott, J., & Freymueller, J. T. (2020). A block model of present-day kinematics of Alaska and western Canada. *Journal of Geophysical Research: Solid Earth*, *125*(7), e2019JB018378. https://doi.org/10.1029/2019JB018378

Endrun, B., Meier, T., Bischoff, M., & Harjes, H. P. (2004). Lithospheric structure in the area of Crete constrained by receiver functions and dispersion analysis of Rayleigh phase velocities. *Geophysical Journal International*, *158*(2), 592–608. https://doi.org/10.1111/j.1365-246X.2004.02332.x

Ergintav, S., Floyd, M., Paradissis, D., Karabulut, H., Vernant, P., Masson, F., et al. (2023). New geodetic constraints on the role of faults and blocks versus distributed strain in the Nubia-Arabia-Eurasia zone of active plate interactions. *Turkish Journal of Earth Sciences*, *32*(3), 248–261. https://doi.org/10.55730/1300-0985.1842

Faccenna, C., Jolivet, L., Piromallo, C., & Morelli, A. (2003). Subduction and the depth of convection in the Mediterranean mantle. *Journal of Geophysical Research*, *108*(B2), 2099. https://doi.org/10.1029/2001JB001690

Faccenna, C., Piromallo, C., Crespo-Blanc, A., Jolivet, L., & Rossetti, F. (2004). Lateral slab deformation and the origin of the western Mediterranean arcs. *Tectonics*, *23*(1), TC1012. https://doi.org/10.1029/2002TC001488

Floyd, M., King, R., Paradissis, D., Karabulut, H., Ergintav, S., Raptakis, K., & Reilinger, R. (2023). Variations in coupling and deformation along the Hellenic subduction zone. *Turkish Journal of Earth Sciences*, *32*(3), 262–274. https://doi.org/10.55730/1300-0985.1843

Fujiwara, T., Kodaira, S., No, T., Kaiho, Y., Takahashi, N., & Kaneda, Y. (2011). The 2011 Tohoku-oki earthquake: Displacement reaching the trench axis. *Science*, *334*(6060), 1240. https://doi.org/10.1126/science.1211554

Ganas, A., & Parsons, T. (2009). Three-dimensional model of Hellenic Arc deformation and origin of the Cretan uplift. *Journal of Geophysical Research*, *114*(B6), B06404. https://doi.org/10.1029/2008JB005599

Gesret, A., Laigle, M., Diaz, J., Sachpazi, M., Charalampakis, M., & Hirn, A. (2011). Slab top dips resolved by teleseismic converted waves in the Hellenic subduction zone. *Geophysical Research Letters*, *38*(20), L20304. https://doi.org/10.1029/2011GL048996

Gudmundsson, Ó., & Sambridge, M. (1998). A regionalized upper mantle (RUM) seismic model. *Journal of Geophysical Research*, *103*(B4), 7121–7136. https://doi.org/10.1029/97JB02488

Guidoboni, E., & Comastri, A. (1997). The large earthquake of 8 August 1303 in Crete: Seismic scenario and tsunami in the Mediterranean area. *Journal of Seismology*, *1*, 55–72. https://doi.org/10.1023/A:1009737632542

Hatzfeld, D. (1994). On the shape of the subducting slab beneath the Peloponnese, Greece. *Geophysical Research Letters*, *21*(3), 173–176. https://doi.org/10.1029/93GL03079

Hayes, G. P., Moore, G. L., Portner, D. E., Hearne, M., Flamme, H., Furtney, M., & Smoczyk, G. M. (2018). Slab2, a comprehensive subduction zone geometry model. *Science*, *362*(6410), 58–61. https://doi.org/10.1126/science.aat4723

Hetland, E. A., & Simons, M. (2010). Post-seismic and interseismic fault creep II: Transient creep and interseismic stress shadows on megathrusts. *Geophysical Journal International*, *181*(1), 99–112. https://doi.org/10.1111/j.1365-246X.2009.04482.x

Howell, A., Jackson, J., England, P., Higham, T., & Synolakis, C. (2015). Late Holocene uplift of Rhodes, Greece: Evidence for a large tsunamigenic earthquake and the implications for the tectonics of the eastern Hellenic Trench system. *Geophysical Journal International*, *203*(1), 459–474. https://doi.org/10.1093/gji/ggv307

Jackson, J., & McKenzie, D. (1988). The relationship between plate motions and seismic tremors, and the rates of active deformation in the Mediterranean and Middle East. *Geophysical Journal International*, *93*(1), 45–73. https://doi.org/10.1111/j.1365-246X.1988.tb01387.x

Jolivet, L., & Brun, J. P. (2010). Cenozoic geodynamic evolution of the Aegean. *International Journal of Earth Sciences*, *99*(1), 109–138. https://doi.org/10.1007/s00531-008-0366-4

Jolivet, L., Faccenna, C., Huet, B., Labrousse, L., Le Pourhiet, L., Lacombe, O., et al. (2013). Aegean tectonics: Strain localisation, slab tearing and trench retreat. *Tectonophysics*, *597*, 1–33. https://doi.org/10.1016/j.tecto.2012.06.011

Kaneko, Y., & Lapusta, N. (2008). Variability of earthquake nucleation in continuum models of rate-and-state faults and implications for aftershock rates. *Journal of Geophysical Research*, *113*(B12), B12312. https://doi.org/10.1029/2007JB005154

Kobayashi, D., La Femina, P., Geirsson, H., Chichaco, E., Abrego, A. A., Mora, H., & Camacho, E. (2014). Kinematics of the western Caribbean: Collision of the cocos ridge and upper plate deformation. *Geochemistry, Geophysics, Geosystems*, *15*(5), 1671–1683. https://doi.org/10.1002/2014GC005234

Konca, A. O., Avouac, J.-P., Sladen, A., Meltzner, A. J., Sieh, K., Fang, P., et al. (2008). Partial rupture of a locked patch of the Sumatra megathrust during the 2007 earthquake sequence. *Nature*, *456*(7222), 631–635. https://doi.org/10.1038/nature07572

Kounoudis, R., Bastow, I. D., Ogden, C. S., Goes, S., Jenkins, J., Grant, B., & Braham, C. (2020). Seismic tomographic imaging of the Eastern mediterranean mantle: Implications for terminal-stage subduction, the uplift of Anatolia, and the development of the North anatolian fault. *Geochemistry, Geophysics, Geosystems*, *21*(7), e2020GC009009. https://doi.org/10.1029/2020GC009009

Kurt, A. I., Özbakir, A. D., Cingoz, A., Ergintav, S., Dogan, U., & Özarpaci, S. (2023). Contemporary velocity field for Turkey inferred from combination of a dense network of long term GNSS observations. *Turkish Journal of Earth Sciences*, *32*(3), 275–293. https://doi.org/10.55730/1300-0985.1844

Le Pichon, X., & Angelier, J. (1979). The Hellenic arc and trench system: A key to the neotectonic evolution of the eastern mediterranean area. *Tectonophysics*, *60*(1–2), 1–42. https://doi.org/10.1016/0040-1951(79)90131-8

Le Pichon, X., & Angelier, J. (1981). The Aegean Sea. *Philosophical Transactions of the Royal Society of London, Series A, Mathematical and Physical Sciences*, *300*(1454), 357–372. https://doi.org/10.1098/rsta.1981.0069

Le Pichon, X., Lallemant, S. J., Chamot-Rooke, N., Lemeur, D., & Pascal, G. (2002). The mediterranean ridge backstop and the Hellenic nappes. *Marine Geology*, *186*(1–2), 111–125. https://doi.org/10.1016/S0025-3227(02)00175-5

Loveless, J. P., & Meade, B. J. (2011). Spatial correlation of interseismic coupling and coseismic rupture extent of the 2011 Mw = 9.0 Tohoku-oki earthquake. *Geophysical Research Letters*, *38*(17), L17306. https://doi.org/10.1029/2011GL048561

Mascle, J., Le Cleac'h, A., & Jongsma, D. (1986). The eastern Hellenic margin from Crete to Rhodes: Example of progressive collision. *Marine Geology*, *73*(1–2), 145–168. https://doi.org/10.1016/0025-3227(86)90116-7

McCaffrey, R. (2009). Time-dependent inversion of three-component continuous GPS for steady and transient sources in northern cascadia. *Geophysical Research Letters*, *36*(7), L07304. https://doi.org/10.1029/2008GL036784

McCaffrey, R. (2014). Interseismic locking on the Hikurangi subduction zone: Uncertainties from slow-slip events. *Journal of Geophysical Research: Solid Earth*, *119*(10), 7874–7888. https://doi.org/10.1002/2014JB010945

McCaffrey, R. (2023). Tdefnode [Software]. *Github*. Retrieved from https://robmccaffrey.github.io/TDEFNODE/TDEFNODE.html

McCaffrey, R., Zwick, P. C., Bock, Y., Prawirodirdjo, L., Genrich, J. F., Stevens, C. W., et al. (2000). Strain partitioning during oblique plate convergence in northern Sumatra: Geodetic and seismologic constraints and numerical modeling. *Journal of Geophysical Research*, *105*(B12), 28363–28376. https://doi.org/10.1029/1999JB900362

McClusky, S., Balassanian, S., Barka, A., Demir, C., Ergintav, S., Georgiev, I., et al. (2000). Global positioning system constraints on plate kinematics and dynamics in the eastern mediterranean and caucasus. *Journal of Geophysical Research*, *105*(B3), 5695–5719. https://doi.org/10.1029/1999JB900351

McGuire, J. J., Plank, T., Barrientos, S. E., Becker, T. W., Brodsky, E., Cottrell, E., et al. (2017). The SZ4D initiative: Understanding the processes that underlie subduction zone hazards in 4D. *Vision document submitted to the National Science Foundation. The IRIS Consortium*. Retrieved from https://www.sz4d.org/_files/ugd/66466d_c5202b9573e1413eb006995304a4b274.pdf

McKenzie, D. (1978). Active tectonics of the Alpine-himalayan belt: The Aegean Sea and surrounding regions. *Geophysical Journal International*, *55*(1), 217–254. https://doi.org/10.1111/j.1365-246X.1978.tb04759.x

Meier, T., Becker, D., Endrun, B., Rische, M., Bohnhoff, M., Stöckhert, B., & Harjes, H. P. (2007). A model for the Hellenic subduction zone in the area of Crete based on seismological investigations. *Geological Society, London, Special Publications*, *291*(1), 183–199. https://doi.org/10.1144/SP291.9

Meier, T., Rische, M., Endrun, B., Vafidis, A., & Harjes, H. P. (2004). Seismicity of the Hellenic subduction zone in the area of western and central Crete observed by temporary local seismic networks. *Tectonophysics*, *383*(3–4), 149–169. https://doi.org/10.1016/j.tecto.2004.02.004

Meijer, P. T., & Wortel, M. J. R. (1997). Present-day dynamics of the Aegean region: A model analysis of the horizontal pattern of stress and deformation. *Tectonics*, *16*(6), 879–895. https://doi.org/10.1029/97TC02004

Menant, A., Sternai, P., Jolivet, L., Guillou-Frottier, L., & Gerya, T. (2016). 3D numerical modeling of mantle flow, crustal dynamics and magma genesis associated with slab roll-back and tearing: The eastern mediterranean case. *Earth and Planetary Science Letters*, *442*, 93–107. https://doi.org/10.1016/j.epsl.2016.03.002

Métois, M., Socquet, A., & Vigny, C. (2012). Interseismic coupling, segmentation and mechanical behavior of the central Chile subduction zone. *Journal of Geophysical Research*, *117*(B3), B03406. https://doi.org/10.1029/2011JB008736

Moreno, M., Rosenau, M., & Oncken, O. (2010). Maule earthquake slip correlates with pre-seismic locking of Andean subduction zone. *Nature*, *467*(7312), 198–202. https://doi.org/10.1038/nature09349

Mouslopoulou, V., Begg, J. G., Polonia, A., Nicol, A., Reston, T. J., Cesca, S., et al. (2025). Hellenic subduction system and upper-plate structures revealed by deep high-resolution seismic-reflection profiles and seafloor bathymetry. *Tectonics*, *44*(9), e2025TC008943. https://doi.org/10.1029/2025TC008943

Mouslopoulou, V., Bocchini, G. M., Cesca, S., Saltogianni, V., Bedford, J., Petersen, G., et al. (2020). Earthquake swarms, slow slip and fault interactions at the western-end of the Hellenic subduction system precede the moment Mw 6.9 Zakynthos earthquake, Greece. *Geochemistry, Geophysics, Geosystems*, *21*(12), e2020GC009243. https://doi.org/10.1029/2020GC009243

Mouslopoulou, V., Nicol, A., Begg, J., Oncken, O., & Moreno, M. (2015). Clusters of megaearthquakes on upper plate faults control the Eastern mediterranean hazard. *Geophysical Research Letters*, *42*(23), 10282–10289. https://doi.org/10.1002/2015gl066371

Moutote, L., Itoh, Y., Lengliné, O., Duputel, Z., & Socquet, A. (2023). Evidence of a transient aseismic slip driving the 2017 Valparaiso earthquake sequence, from foreshocks to aftershocks. *Journal of Geophysical Research: Solid Earth*, *128*(9), e2023JB026603. https://doi.org/10.1029/2023JB026603

Murray-Moraleda, J. (2009). GPS: Applications in crustal deformation monitoring. In R. A. Meyers (Ed.), *Encyclopedia of complexity and systems science* (pp. 4249–4283). Springer. https://doi.org/10.1007/978-0-387-30440-3_250

Nocquet, J.-M., Jarrin, P., Vallee, M., Mothes, P. A., Grandin, R., Rolandone, F., et al. (2017). Supercycle at the Ecuadorian subduction zone revealed after the 2016 Pedernales earthquake. *Nature Geoscience*, *10*(2), 145–149. https://doi.org/10.1038/ngeo2864

Noda, H., & Lapusta, N. (2013). Stable creeping fault segments can become destructive as a result of dynamic weakening. *Nature*, *493*(7433), 518–521. https://doi.org/10.1038/nature11703

Ohta, Y., Kimata, F., & Sagiya, T. (2004). Reexamination of the interplate coupling in the Tokai region, central Japan, based on the GPS data in 1997-2002. *Geophysical Research Letters*, *31*(24), L24604. https://doi.org/10.1029/2004GL021404

Okada, Y. (1992). Internal deformation due to shear and tensile faults in a half-space. *Bulletin of the Seismological Society of America*, *82*(2), 1018–1040. https://doi.org/10.1785/BSSA0820021018

Ott, R. F., Wegmann, K. W., Gallen, S. F., Pazzaglia, F. J., Brandon, M. T., Ueda, K., & Fassoulas, C. (2021). Reassessing Eastern mediterranean tectonics and earthquake hazard from the 365 CE earthquake. *AGU Advances*, *2*, e2020AV000315. https://doi.org/10.1029/2020AV000315

Özbakir, A. D., Şengör, A. M. C., Wortel, M. J. R., & Govers, R. (2013). The Pliny-Strabo trench region: A large shear zone resulting from slab tearing. *Earth and Planetary Science Letters*, *375*, 188–195. https://doi.org/10.1016/j.epsl.2013.05.025

Papadimitriou, P., Kapetanidis, V., Karakonstantis, A., Spingos, I., Pavlou, K., Kaviris, G., et al. (2021). The 25 October 2018 Zakynthos (greece) earthquake: Seismic activity at the transition between a transform fault and a subduction zone. *Geophysical Journal International*, *225*(1), 15–36. https://doi.org/10.1093/gji/ggaa575

Papazachos, B. C., Karakostas, V. G., Papazachos, C. B., & Scordilis, E. M. (2000). The geometry of the Wadati-Benioff zone and lithospheric kinematics in the Hellenic arc. *Tectonophysics*, *319*(4), 275–300. https://doi.org/10.1016/S0040-1951(99)00299-1

Pearce, F. D., Rondenay, S., Sachpazi, M., Charalampakis, M., & Royden, L. H. (2012). Seismic investigation of the transition from continental to oceanic subduction along the western Hellenic subduction zone. *Journal of Geophysical Research*, *117*(B7), B07306. https://doi.org/10.1029/2011JB009023

Perry, M., Muller, C., Protti, M., Feng, L., & Hill, E. M. (2025). Interseismic magathrust coupling at the Osa peninsula, Costa Rica. *Journal of Geophysical Research: Solid Earth*, *130*(7), e2024JB030641. https://doi.org/10.1029/2024JB030641

Piromallo, C., & Morelli, A. (2003). P wave tomography of the mantle under the Alpine-Mediterranean area. *Journal of Geophysical Research*, *108*(B2). https://doi.org/10.1029/2002JB001757

Pondrelli, S. (2002). European-mediterranean regional centroid-moment tensors catalog (RCMT). *Istituto Nazionale di Geofisica e Vulcanologia (INGV)*. [Dataset]. https://doi.org/10.13127/rcmt/euromed

Protti, M., González, V., Newman, A., Dixon, T. H., Schwartz, S. Y., Marshall, J. S., et al. (2014). Nicoya earthquake rupture anticipated by geodetic measurement of the locked plate interface. *Nature Geosciences*, *7*(2), 117–121. https://doi.org/10.1038/ngeo2038

Radiguet, M., Perfettini, H., Cotte, N., Gualandi, A., Valette, B., Kostoglodov, V., et al. (2016). Triggering of the 2014 Mw7.3 papanoa earthquake by a slow slip event in Guerrero, Mexico. *Nature Geoscience*, *9*(11), 829–833. https://doi.org/10.1038/ngeo2817

Reilinger, R., McClusky, S., Paradissis, D., Ergintav, S., & Vernant, P. (2010). Geodetic constraints on the tectonic evolution of the Aegean region and strain accumulation along the Hellenic subduction zone. *Tectonophysics*, *488*(1–4), 22–30. https://doi.org/10.1016/j.tecto.2009.05.027

Reilinger, R., McClusky, S., Vernant, P., Lawrence, S., Ergintav, S., Cakmak, R., et al. (2006). GPS constraints on continental deformation in the Africa-Arabia-Eurasia continental collision zone and implications for the dynamics of plate interactions. *Journal of Geophysical Research*, *111*(B5), B05411. https://doi.org/10.1029/2005JB004051

Ring, U., Glodny, J., Will, T., & Thomson, S. (2010). The Hellenic subduction system: HighPressure metamorphism, exhumation, normal faulting, and large-scale extension. *Annual Review of Earth and Planetary Sciences*, *38*(1), 45–76. https://doi.org/10.1146/annurev.earth.050708.170910

Rolandone, F., Nocquet, J.-M., Mothes, P. A., Jarrin, P., Vallée, M., Cubas, N., et al. (2018). Areas prone to slow slip events impede earthquake rupture propagation and promote afterslip. *Science Advances*, *4*(1), eaao6596. https://doi.org/10.1126/sciadv.aao6596

Rondenay, S., Abers, G. A., & van Keken, P. E. (2008). Seismic imaging of subduction zone metamorphism. *Geology*, *36*(4), 275–278. https://doi.org/10.1130/G24112A.1

Royden, L. H. (1993). Evolution of retreating subduction boundaries formed during continental collision. *Tectonics*, *12*(3), 629–638. https://doi.org/10.1029/92TC02641

Royden, L. H., & Papanikolaou, D. J. (2011). Slab segmentation and late Cenozoic disruption of the Hellenic arc. *Geochemistry, Geophysics, Geosystems*, *12*(3), Q03010. https://doi.org/10.1029/2010GC003280

Saffer, D. M., & Tobin, H. J. (2011). Hydrogeology and mechanics of subduction zone forearcs: Fluid flow and pore pressures. *Annual Review of Earth and Planetary Sciences*, *39*(1), 157–186. https://doi.org/10.1146/annurev-earth-040610-133408

Saltogianni, V., Mouslopoulou, V., Dielforder, A., Bocchini, G. M., Bedford, J., & Oncken, O. (2021). Slow slip triggers the 2018 M_w 6.9 Zakynthos earthquake within the weakly locked Hellenic subduction system, Greece. *Geochemistry, Geophysics, Geosystems*, *22*(11), e2021GC010090. https://doi.org/10.1029/2021GC010090

Saltogianni, V., Mouslopoulou, V., Oncken, O., Nicol, A., Gianniou, M., & Mertikas, S. (2020). Elastic fault interactions and earthquake rupture along the southern Hellenic subduction plate interface zone in Greece. *Geophysical Research Letters*, *47*(13), e2019GL086604. https://doi.org/10.1029/2019GL086604

Schildgen, T. F., Yildirim, C., Cosentino, D., & Strecker, M. R. (2014). Linking slab break-off, Hellenic trench retreat, and uplift of the central and eastern Anatolian plateaus. *Earth-Science Reviews*, *128*, 147–168. https://doi.org/10.1016/j.earscirev.2013.11.006

Scholz, C. H. (2019). *The mechanics of earthquakes and faulting*. Cambridge University Press. https://doi.org/10.1017/9781316681473

Shaw, B., Ambraseys, N. N., England, P. C., Floyd, M. A., Gorman, G. J., Higham, T. F. G., et al. (2008). Eastern mediterranean tectonics and tsunami hazard inferred from the AD 365 earthquake. *Nature Geoscience*, *1*(4), 268–276. https://doi.org/10.1038/ngeo151

Shaw, B., & Jackson, J. (2010). Earthquake mechanisms and active tectonics of the Hellenic subduction zone. *Geophysical Journal International*, *181*, 966–984. https://doi.org/10.1111/j.1365-246X.2010.04551.x

Socquet, A., Valdes, J. P., Jara, J., Cotton, F., Walpersdorf, A., Cotte, N., et al. (2017). An 8 month slow slip event triggers progressive nucleation of the 2014 Chile megathrust. *Geophysical Research Letters*, *44*(9), 4046–4053. https://doi.org/10.1002/2017GL073023

Sodoudi, F., Kind, R., Hatzfeld, D., Priestley, K., Hanka, W., Wylegalla, K., et al. (2006). Lithospheric structure of the Aegean obtained from P and S receiver functions. *Journal of Geophysical Research*, *111*(B12), B12307. https://doi.org/10.1029/2005JB003932

Spakman, W., Wortel, M. J. R., & Vlaar, N. J. (1988). The Hellenic subduction zone: A tomographic image and its geodynamic implications. *Geophysical Research Letters*, *15*(1), 60–63. https://doi.org/10.1029/GL015i001p00060

Suckale, J., Rondenay, S., Sachpazi, M., Charalampakis, M., Hosa, A., & Royden, L. H. (2009). High-resolution seismic imaging of the western Hellenic subduction zone using teleseismic scattered waves. *Geophysical Journal International*, *178*(2), 775–791. https://doi.org/10.1111/j.1365-246X.2009.04170.x

Symithe, S., Calais, E., de Chabalier, J. B., Robertson, R., & Higgins, M. (2015). Current block motions and strain accumulation on active faults in the Caribbean. *Journal of Geophysical Research: Solid Earth*, *120*(5), 3748–3774. https://doi.org/10.1002/2014JB011779

Taymaz, T., Jackson, J., & McKenzie, D. (1991). Active tectonics of the north and central Aegean Sea. *Geophysical Journal International*, *106*(2), 433–490. https://doi.org/10.1111/j.1365-246X.1991.tb03906.x

Taymaz, T., Jackson, J., & Westaway, R. (1990). Earthquake mechanisms in the Hellenic Trench near Crete. *Geophysical Journal International*, *102*(3), 695–731. https://doi.org/10.1111/j.1365-246X.1990.tb04590.x

ten Veen, J. H., & Kleinspehn, K. L. (2003). Incipient Continental collision and plate-boundary curvature: Late Pliocene-Holocene transtensional Hellenic forearc, Crete, Greece. *Journal of the Geological Society*, *160*(2), 161–181. https://doi.org/10.1144/0016-764902-067

Vaněk, J., Hanuš, V., Christova, C., & Simeonova, S. (1987). Morphology of the Wadati-Benioff zone in the Hellenic arc. *Journal of Geodynamics*, *8*(1), 79–93. https://doi.org/10.1016/0264-3707(87)90059-7

van Hinsbergen, D. J. J., Kaymakci, N., Spakman, W., & Torsvik, T. H. (2010). Reconciling the geological history of western Turkey with plate circuits and mantle tomography. *Earth and Planetary Science Letters*, *297*(3–4), 674–686. https://doi.org/10.1016/j.epsl.2010.07.024

van Hinsbergen, D. J. J., & Schmid, S. M. (2012). Map view restoration of Aegean–West Anatolian accretion and extension since the Eocene. *Tectonics*, *31*(5), TC5005. https://doi.org/10.1029/2012tc003132

Vernant, P., Reilinger, R., & McClusky, S. (2014). Geodetic evidence for low coupling on the Hellenic subduction plate interface. *Earth and Planetary Science Letters*, *385*, 122–129. https://doi.org/10.1016/j.epsl.2013.10.018

Wallace, L. M., Barnes, P., Beavan, J., Van Dissen, R., Litchfield, N., Mountjoy, J., et al. (2012). The kinematics of a transition from subduction to strike-slip: An example from the central New Zealand plate boundary. *Journal of Geophysical Research*, *117*(B2), B02405. https://doi.org/10.1029/2011JB008640

Wallace, L. M., Beavan, J., McCaffrey, R., & Darby, D. (2004). Subduction zone coupling and tectonic block rotations in the North Island, New Zealand. *Journal of Geophysical Research*, *109*(B12), B12406. https://doi.org/10.1029/2004JB003241

Wallace, P. J. (2005). Volatiles in subduction zone magmas: Concentrations and fluxes based on melt inclusion and volcanic gas data. *Journal of Volcanology and Geothermal Research*, *140*(1–3), 217–240. https://doi.org/10.1016/j.jvolgeores.2004.07.023

Wessel, P., Luis, J. F., Uieda, L., Scharroo, R., Wobbe, F., Smith, W. H. F., & Tian, D. (2019). The generic mapping tools version 6. *Geochemistry, Geophysics, Geosystems*, *20*(11), 5556–5564. https://doi.org/10.1029/2019GC008515

Wirth, E. A., Sahakian, V. J., Wallace, L. M., & Melnick, D. (2022). The occurrence and hazards of great subduction zone earthquakes. *Nature Reviews Earth & Environment*, *3*(2), 125–140. https://doi.org/10.1038/s43017-021-00245-w

Wortel, M. J. R., & Spakman, W. (2000). Subduction and slab detachment in the Mediterranean-Carpathian region. *Science*, *290*(5498), 1910–1917. https://doi.org/10.1126/science.290.5498.1910